Design concepts for primary mirror support structures of large telescopes for optical and submillimeter astronomy

Christian L. Stutzki,[a] Hiroki Tamai,[a] Thomas A. Sebring[b]
[a] Stutzki Engineering, Inc.,
338 North Milwaukee Street, Suite 101, Milwaukee WI, USA 53202;
[b] Center for Radiophysics and Space Research,
Cornell Univ., Ithaca, NY USA 14853

Design concepts for primary mirror support structures of large telescopes for optical and submillimeter astronomy

Christian L. Stutzki *[a], Hiroki Tamai[a], Thomas A. Sebring[b]

[a]Stutzki Engineering, Inc., 338 North Milwaukee Street, Suite 101, Milwaukee WI, USA 53202;
[b] Center for Radiophysics and Space Research, Cornell Univ., Ithaca, NY USA 14853

ABSTRACT

Technologies of modern optical and submillimeter telescopes with large primary mirror are based on adaptive optics. These telescopes operate with many small mirror segments, so that all the segments work as a large piece of a reflective curved plate, i.e. a paraboloid. Each mirror segment is independently attached to a support structure via adjustable warping harnesses. A support structure is required to be extremely rigid in order to maintain the reflective surface. This paper describes the conceptual approach for the design of such support structures. A system proven to fulfill these requirements with efficient structural material use is a node-and-bar system, so-called space frame. The rules for geometry of space frame structures are based on the system of the five 'platonic solids': The edges of the conceptually assembled solids can be replaced by the bar members of a space frame to achieve maximum stiffness. This conceptual approach is demonstrated with examples in the paper, by illustrating the determination of the geometry and examining the deformation due to the telescope rotations during operation. This paper also demonstrates design solutions for other issues relevant to space frame geometry, such as effects of gradient thermal load and redundancy of the structures.

Keywords: optical telescope, space frame structure, platonic solids, design concept

1. INTRODUCTION

This paper presents the development of stable and rigid space frame geometries as well as the application to a 25 meter large truss for the primary mirror of an optical telescope. The ideal requirement of infinite stiffness and zero deformation during the rotation of the telescope cannot be fulfilled due to the elastic nature of materials. But the stiffness can be optimized, reducing the deflections between two extreme positions to L/5000 (L being the span or diameter of the truss). Just as a comparison: normal buildings require L/250 deflection limits, which is accomplished with much more material than the L/5000 in the current example for the telescope. In addition the requirements are to be lightweight, easy to ship, and easy to assemble. Only space frames can accomplish this required performance.

2. DESIGN CONCEPTS

2.1 Platonic solids and space frame structure

A spaceframe can be conceived as an assembly of bars and "nodes", but also as an assembly of Platonic bodies (Fig. 1). The classic space frame geometry is developed from semi-octahedrons and tetrahedrons as shown in Fig.2.
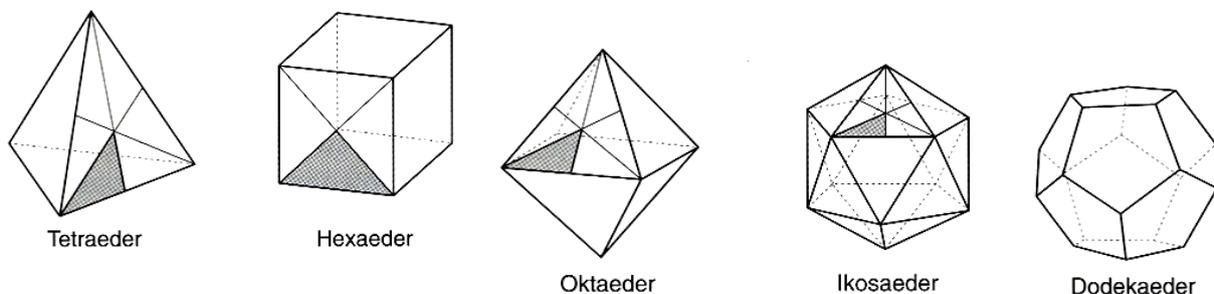

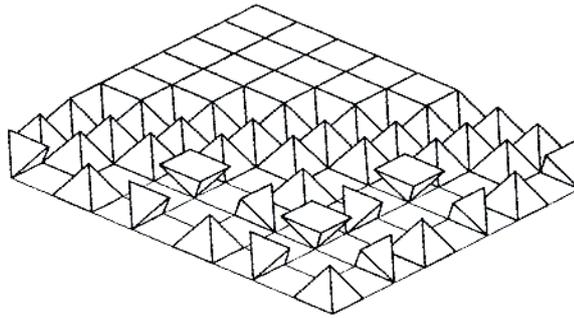Fig. 1. The five basic Platonic bodies

Fig.2. Composition of a slab-shaped, rectangular spatial framework consisting of semi- octahedrons and tetrahedrons

The stability of a space frame is defined as follows: a free spatial truss is stable (rigid, non- kinematic) if, and only if the Jacobian determinant of the order s = 3k-6 for the implicit functions of the squares of distances between the nodes is non-zero, with s being the number of bars, and k being the number of nodes.

With the words of Johann Wolfgang von Goethe "architecture is frozen music", the space frame can be conceived as a structural composition. The rules for composing space frames with the help of the basic Platonic bodies were summarized by Foeppl [1], Mengeringhausen [2], and Klimke [3]. The authors developed the CCAT schemes based on these rules, but the project related "reality test" is then done with the computerized truss analysis. However this analysis is only one tool to optimize rigidity. Another one is to arrange the stable sub-frames or "Platonic bodies" in such way that the forces are flowing evenly through the whole system, avoiding stress concentrations and "bottle necks "of load transfer.

2.2 Relevant design issues

Although redundancy is a desirable goal in building structures in general, in the case of a highly redundant space frame structure, this leads to an accumulation of fabrication or construction tolerances, which may cause considerable residual stress. It may end up with misfits and gaps in the bolted connections in the worst case. In addition, significant self-straining effects are anticipated by thermal change, notably gradient thermal load, because of the high redundancy. These issues can be resolved by reducing degree of connectivity in node-and-bar configuration while maintaining structural stability and the stiffness required [4]. Thus the optimization is driven by the rules of composition to achieve stability, by the arrangement of the sub-structures to achieve an even flow of forces, and by the desire to reduce the redundancy of the system without reducing the rigidity. These steps can be followed by comparing Scheme 1 and Scheme 2 in the example below, with Scheme 2 evolving towards a better fulfillment of the requirements.

Another aspect of the space frame concept for the circular telescope truss is the desire to achieve symmetries. The mirror arrangement has a symmetry number of 3. The support structure has a symmetry of 2. The intermediate space frame plane gets a symmetry of 6. The geometries from the mirror level down to the support structure are therefore close to be equal, but because of a lack of higher symmetries, the shapes vary slightly from module to module.

3. DESIGN EXAMPLES

3.1 Design requirement and specifications

This section demonstrates the design of the primary mirror trusses and discusses their structural performance. The following tow examples are the schemes investigated for Cornell Caltech Atacama Telescope project, CCAT. The geometric requirements for the support structure of this submillimeter telescope were following; 1. The coordinates of 210 front surface nodes (actuators) in CCAT mirror truss were provided by JPL. These nodes are located on a paraboloid surface (Fig 3). 2. Theoretical lowest point of this mirror paraboloid must be located three meter off from the tertiary mirror drive (or axis of the hub shaft). 3. The minimum distance from mirror segment to joints of centerlines of bar members is found to be 300 mm (< 103mm mirror + 150mm actuator + half the ball joint diameter).
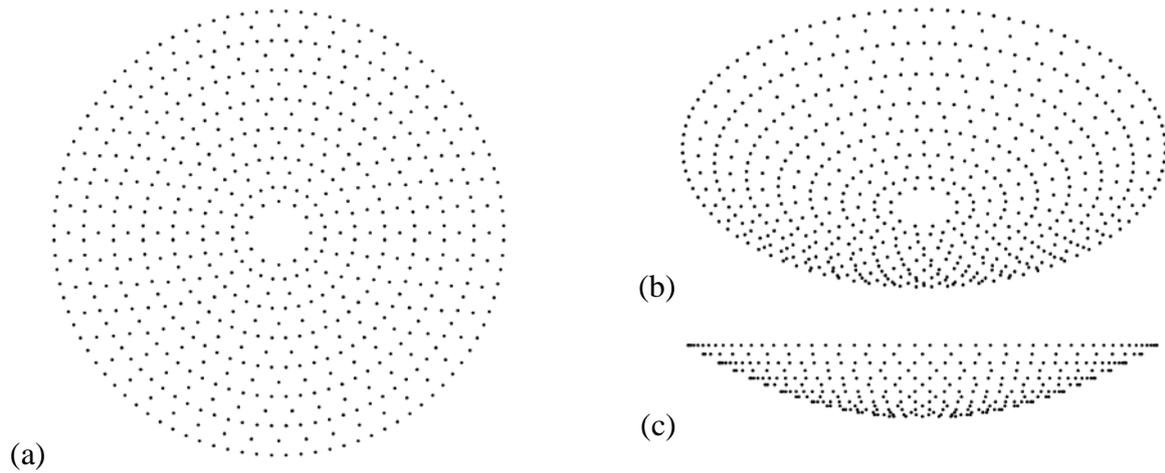
Fig. 3. Nodes of Front Surface of the Space Frame Provided by JPL: (a) Plan, (b) Bird view, (c) Elevation

The expected controlling load cases are dead load and thermal load. Superimposed loads assumed are 10kg/m^2 for mirror segments and 3kg for each actuator. In operations of the telescope, the effects of dead loads are varied due to the tilt angle of the mirror axis, ranging from zenith pointing to horizon pointing. In this paper, tilt angle is measured from the zenith direction such that zenith pointing state, in which the primary mirror is horizontally laid, is referred to as 0 degree position and the most horizon pointing state is referred to as 75 degree position, in which the primary mirror is steeply elevated. Two extreme cases, 0 and 75 degree cases were investigated. In order to simulate effects of different temperature, four scenarios described in Table 2 were calculated. In all four cases the temperature of the supporting octagon is kept unchanged (= 0°C). The actual temperature gradients can be simulated by factorizing and superimposing these 4 basic cases.

Table 1. Applied load cases

DL1	Dead load in the zenith pointing position, i.e. the primary mirror axis is vertical (0 degree).
DL2	Dead load in the horizon pointing position, in which the primary mirror axis is the most tilted (75 degree).
TL1	Uniform temperature of all space frame members of 100oC
TL2	Temperature gradient from left to right, applied in 5 zones. Each zone is an approximately 5 meter wide strip, and all members in this zone have the same temperature level. Zone 1 is 20oC, Zone 2 is 40oC, Zone 3 60oC, zone 4 is 80oC, and zone 5 is 100oC.
TL3	Temperature gradient from bottom to top. This is not done along the z- coordinate, but by layer. Layer 3 (bottom layer) is 20oC, the intermediate layer 2-3 is 40oC, layer 2 is 60oC, layer 2-1 is 80oC, layer 1 (top layer) is 100oC.
TL4	temperature of the long bracing members only, 100oC

Deformation and natural frequency of the structure are required to be carefully controlled: Relative deflection of all front surface nodes required being less than 5 mm, and a natural frequency higher than 5 Hz is preferred.

For the structural analysis, the entire tubular space frame is modeled only with truss elements, which carry only axial force. The mirror segments and adjustment device is simulated by mass elements that stand off from the front surface of the primary truss by 0.25 meters, to the centroid of the mirror segment. Three fictitious truss members are added to represent the rigid offset from the structural center lines.

3.2 CCAT Scheme 1

The structural system used is a space frame type with spherical joints, and tubular members connected to the joints with bolts. The shape is a concave disk consisting of a space frame with three chord layers. The sectional diagram in Fig.4 shows the typical dimensions and concept of installing the primary truss on the octagonal hub. The first layer is closest to the mirror, the third one is at the bottom attached to the octagonal hub, and the second one is in between. Each chord layer is connected with diagonals to its adjacent chord layers. This primary mirror truss is supported at 17 points on the octagonal hub, as shown by circles in Fig.5 (d). The third layer is directly supported by the octagonal hub at eight points on the second innermost ring, while eight outriggers connect eight points on the middle ring of the third layer to the rest nine points on the octagonal hub. The outriggers are illustrated in red. In order to increase the stiffness of the space frame while keeping consistency of the geometry, suggestion was made that the top surface level of the octagonal hub should be lowered by 0.35 meters. Carbon steel A36 or equivalent was assumed for material, and reduced modulus of elasticity, 200 GPa instead of 205 GPa was used to take into account

anticipated looseness of joints for preliminary design purpose; more accurate evaluations of all joints are needed for the next design phase. The diameter of the steel bar members is 60 mm and 76 mm. The generation of the geometry was done in such a way that nowhere in the structure there are angles less than 40 degrees, so the node diameters (which depend on the angles between adjacent members) can be reasonably small. Fig.5 illustrates the configuration of the three layers of the space frame, and the conceptual approach is summarized in Table 2. Fig 6 shows computer-rendered structural model of the space frame from various angles.
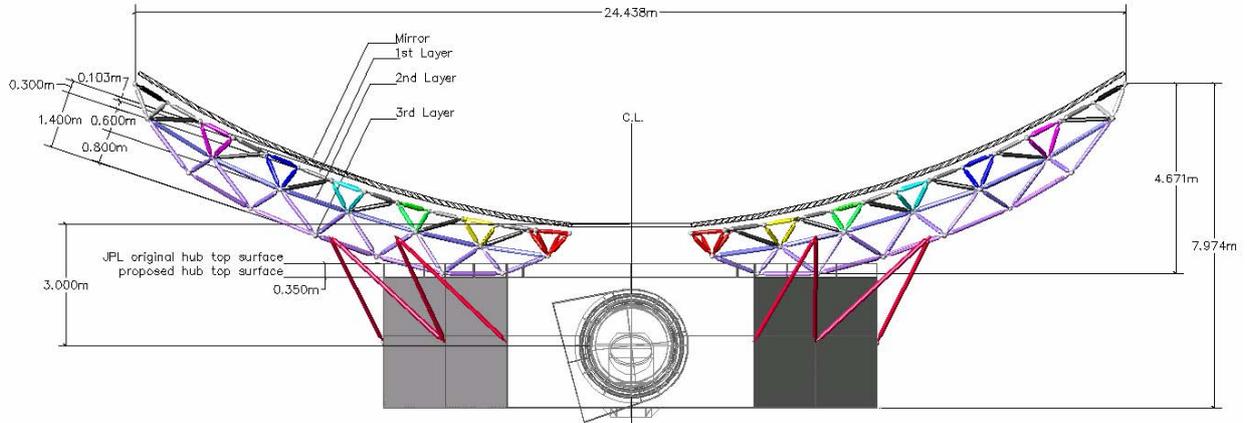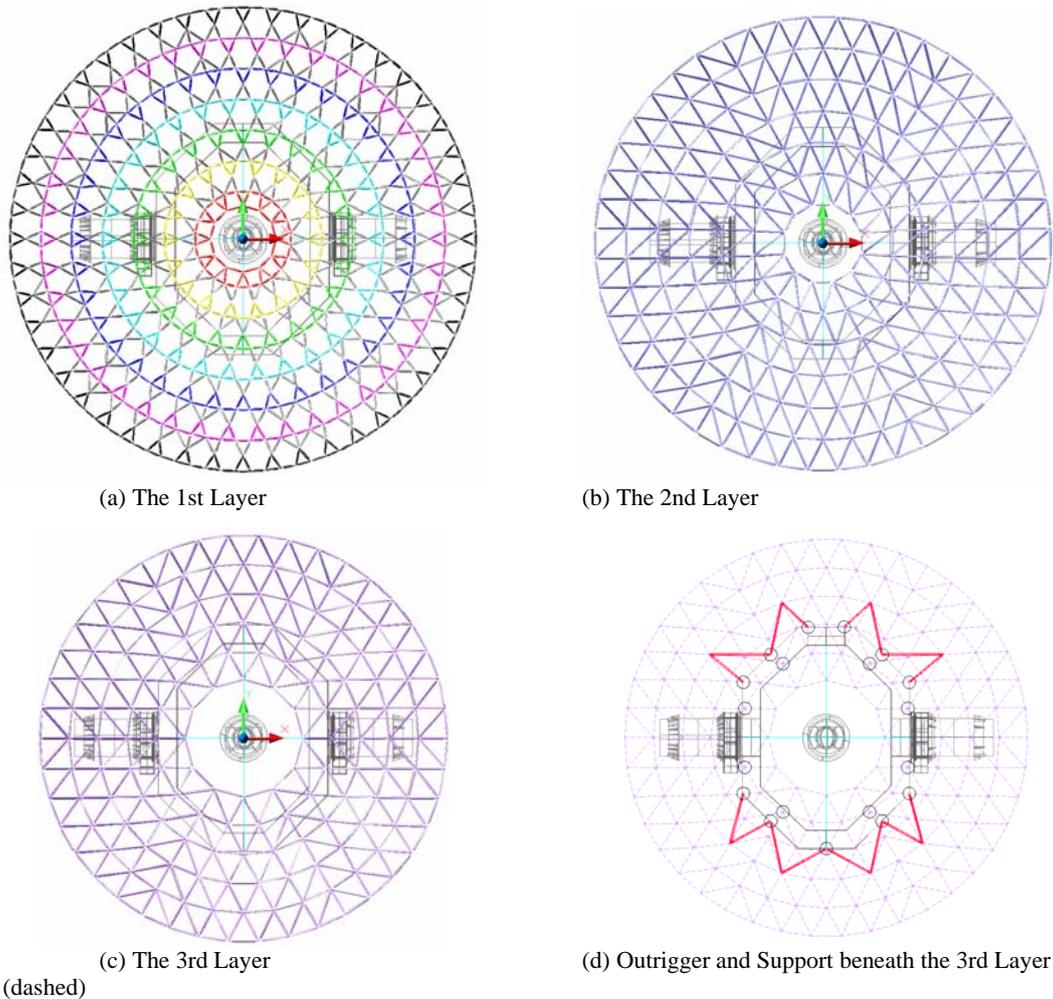

Fig. 4. Sectional Diagram

(a) The 1st Layer

(b) The 2nd Layer

(c) The 3rd Layer (dashed)
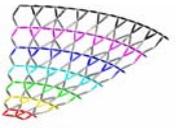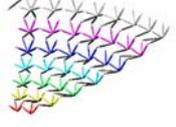

(d) Outrigger and Support beneath the 3rd Layer
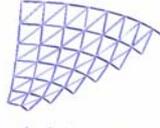
Fig. 5. Projected Plans of the Space Frame Layers (Scheme 1)

Table 2. Configuration diagram of 1/6 space frame (Scheme 1).

	The 1st Layer	The smallest module of the triangulation, primary triangle, of the space frame was determined by the modules for mirror segments provided by JPL. These small triangles must be linked each other in both radial and tangent direction by other space frame members, which form a regular pattern of quadrangular, pentagonal and hexagonal regions.
	Diagonals between the 1st and 2nd Layers	The diagonals are deployed beneath the non-triangular regions of the 1st layer. The equal colors indicate equal lengths. Three brace member are added to stabilize the outermost ring.
	The 2nd Layer	The nodes of this layer were determined to be the center points of the spheres that are defined by adjacent four nodes of adjacent two primary triangles. Distance from the upper layer is determined to avoid undesired shallow angles in relation to the chord layers.
	Diagonals between the 2nd and 3rd Layers	Three members were assigned to support one node in the above layer.
	The 3rd Layer	This layer has the least constraints from the 1st layer. Thus it could be optimized in a way that the members in all rings have equal length.
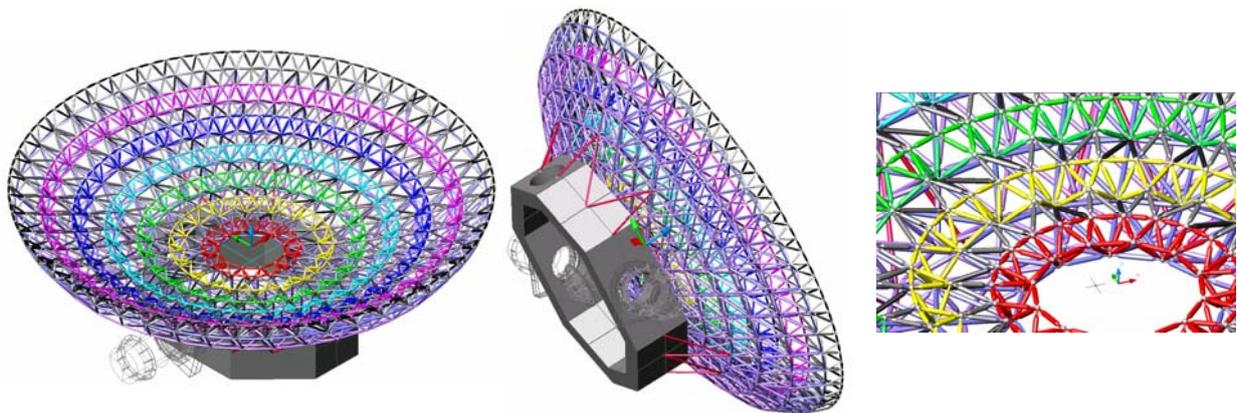
g. 6. Computer rendering images of primary mirror support structure (Scheme 1)

To meet the structural performance requirement, the pipe sections with diameters of 60 mm and 76 mm are selected for bar members. The member sizes are determined by the stiffness of the structure rather than strength of the members. Thus, stress capacities of all the members were found sufficient: actual stress ratios to the strength capacity of the members are less than 30 %. For the connection of the space frame, ball joints with nominal diameter of 132 millimeter are assumed to be assigned to the whole structure. The total truss weight of this scheme is around 31 to 33 metric tons.

Fig.7 and Fig.8 illustrates the over all deformation of the primary truss with a scale factor of 500. It shows neither global nor local instability. In zenith pointing position, the maximum displacement magnitude is found 3.45 millimeters, which causes the maximum vertical deflection, 3.15 millimeter, of the fringes that are seen as the largest overhang situations. The vertical deflections are dominant component of the magnitudes. U1 direction, in which direction the octagonal hub is narrower, is the second dominant. From the figures (a), more than 90 % of the surface displaced less than 2.5 millimeters.

In horizon pointing position, similar structural behaviors can be observed except that the tilt angle causes the rotation of the primary truss. The maximum displacement magnitude is 3.73 millimeters, which causes the maximum rotation of 0.0143 degree about the axis of hub shaft.
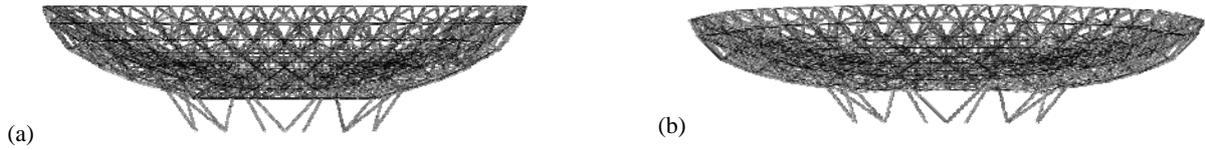
Fig. 7. Deformation due to gravity in Case 0 degree (Scheme 1) (a) Initial state (b) deformed state
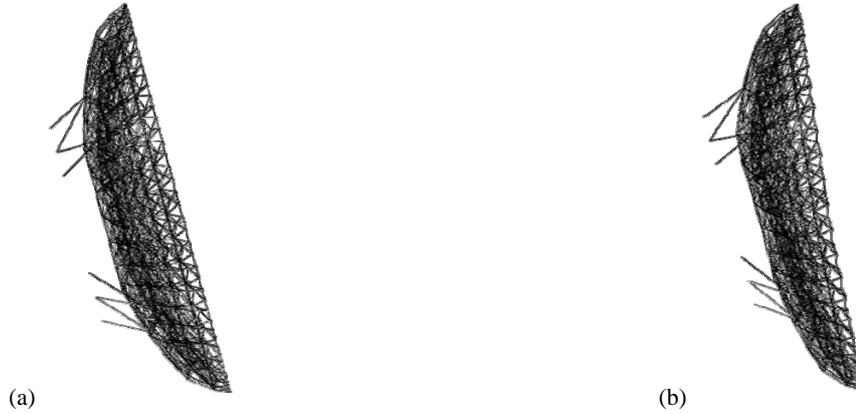

Fig. 8. Deformation due to gravity in Case 75 degree (Scheme 1) (a) Initial state (b) deformed state

Relative displacements of the front surface nodes from 0 degree case to 75 degree case are shown in Figure 14 with a displacement scale factor of 200 and summarized in Table 2. The initial, i.e. undeformed, geometry of front nodal surface is drawn in gray lines as reference. The displacement geometry shown in red represents differential displacement due to gravity in 0 degree position and 75 degree position. To clarify, the differential displacement vector du in this paper is defined as following;

$$du = u_{75} - u_0$$

, where u_{75} is the displacement vector of front surface nodes due to gravity in Case 75 Degree, and u_0 is that of Case 0 Degree. The contours in Fig 9 visualize the relative displacement of the front nodes of the primary truss and following mirror surface. In this analysis, the plate elements to represent the mirror surface were defined only for visualization purpose as non-structural elements, i.e. no stiffness is specified, so that the surface simply follow the deformation of the 1st layer the space frame. As shown in the Table 3, the maximum relative deflections in any position between an angle between 0 and 75 degrees are around 4 mm.
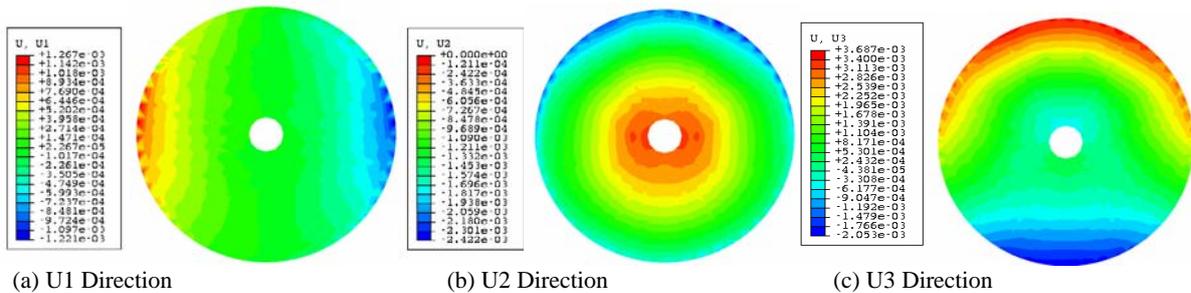

(a) U1 Direction (b) U2 Direction (c) U3 Direction

Fig. 9. Relative deformation of the 1st layer (Scheme 1)

Table 3. Relative displacement due to gravity of Case 75 degree to Case 0 degree (Scheme 1)

Scheme 1	displacement vector (mm)		
	dx	dy	dz
max	1.43	-0.19	4.12
min	-1.37	-2.72	-2.29

The results of thermal load analysis are summarized in Table 4. To obtain displacement due to one Celsius degree increment, the value in Table 4 need to be divided by one hundred. The mirror surface deformations due to two thermal loads are illustrated in Fig.10. The natural frequency modes of the structure were calculated. The lowest natural frequency is around 7 Hz. The first four modes and frequency are shown in Fig. 11.

Table 4. Displacement Due to Temperature Gradients (Scheme 1)

direction	TL1 displacement (mm)			TL2 displacement (mm)			TL3 displacement (mm)			TL4 displacement (mm)		
	dx	dy	dz	dx	dy	dz	dx	dy	dz	dx	dy	dz
max	19.0	14.9	10.8	15.4	10.4	6.9	19.3	19.0	2.8	2.1	3.8	9.2
min	-19.1	-14.7	-8.7	-8.0	-10.4	-5.5	-19.3	-19.2	-17.0	-2.2	-3.1	-2.0
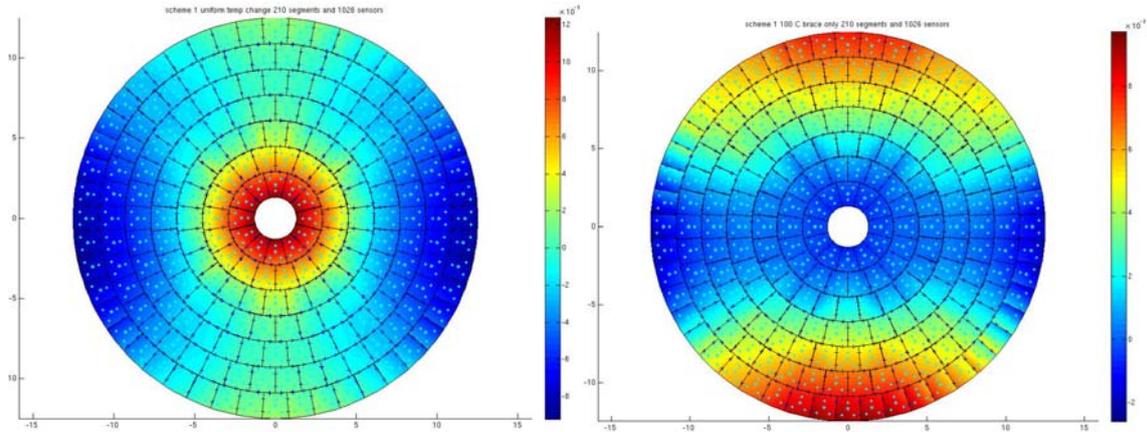
Fig. 10. Deformation due to temperature (Scheme 1)

(a) Mode 1 (7.14 Hz)

(b) Mode 2 (7.51 Hz)
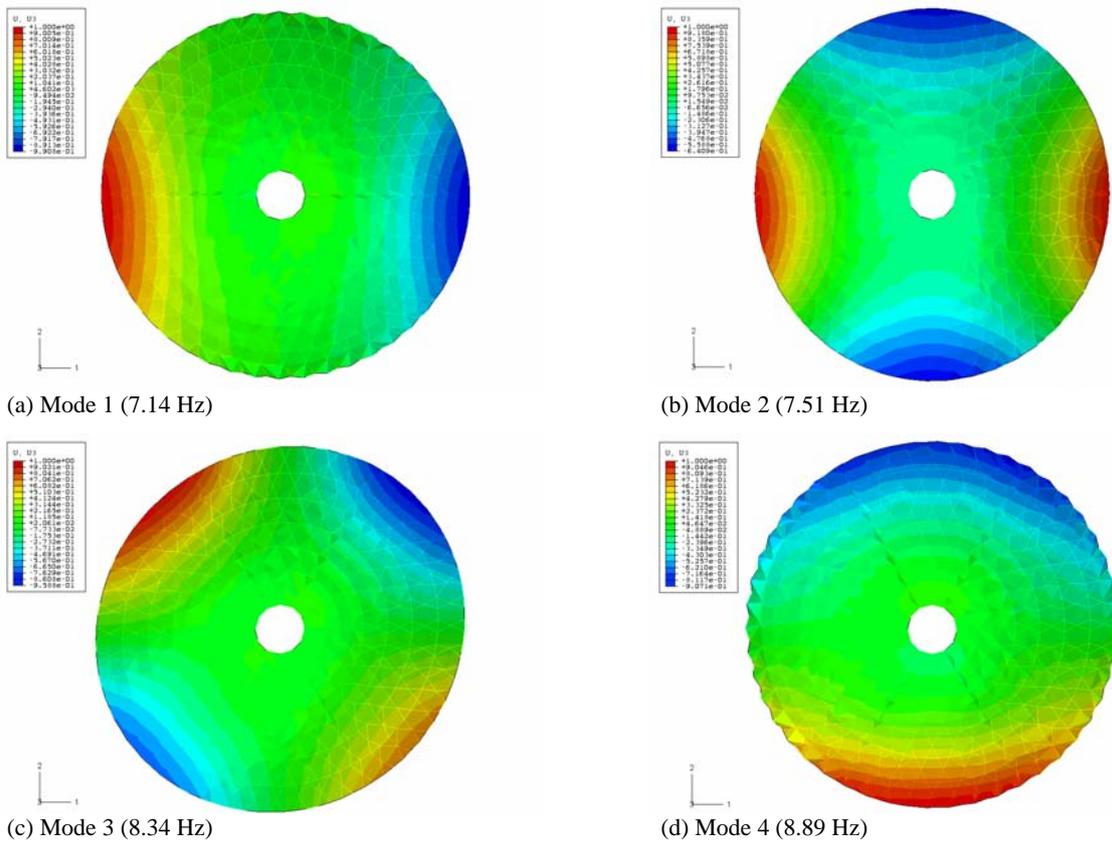
(c) Mode 3 (8.34 Hz)

(d) Mode 4 (8.89 Hz)

Fig. 11. Natural vibration modes and frequencies (Scheme 1)

3.3 CCAT Scheme 2

Scheme 2 is based on Scheme 1 with the following modifications: Instead of a fully triangulated truss system, this is a semi-sparse system consisting of 2892 members, which is about 1/3 reduction in number of bar members. See Fig 12 and Fig 13. The truss weight is reduced to about 24 metric tons. A comparison of layers Table 2 and table 5 shows the apparent difference in space fram configuration. This results in approximately 10% loss of stiffness (Fig. 14 and Fig 15), but allows a lower grade of redundancy. Lower redundancy is desirable in order to avoid high residual stress and potential misfits due to accumulation of fabrication and construction tolerance.
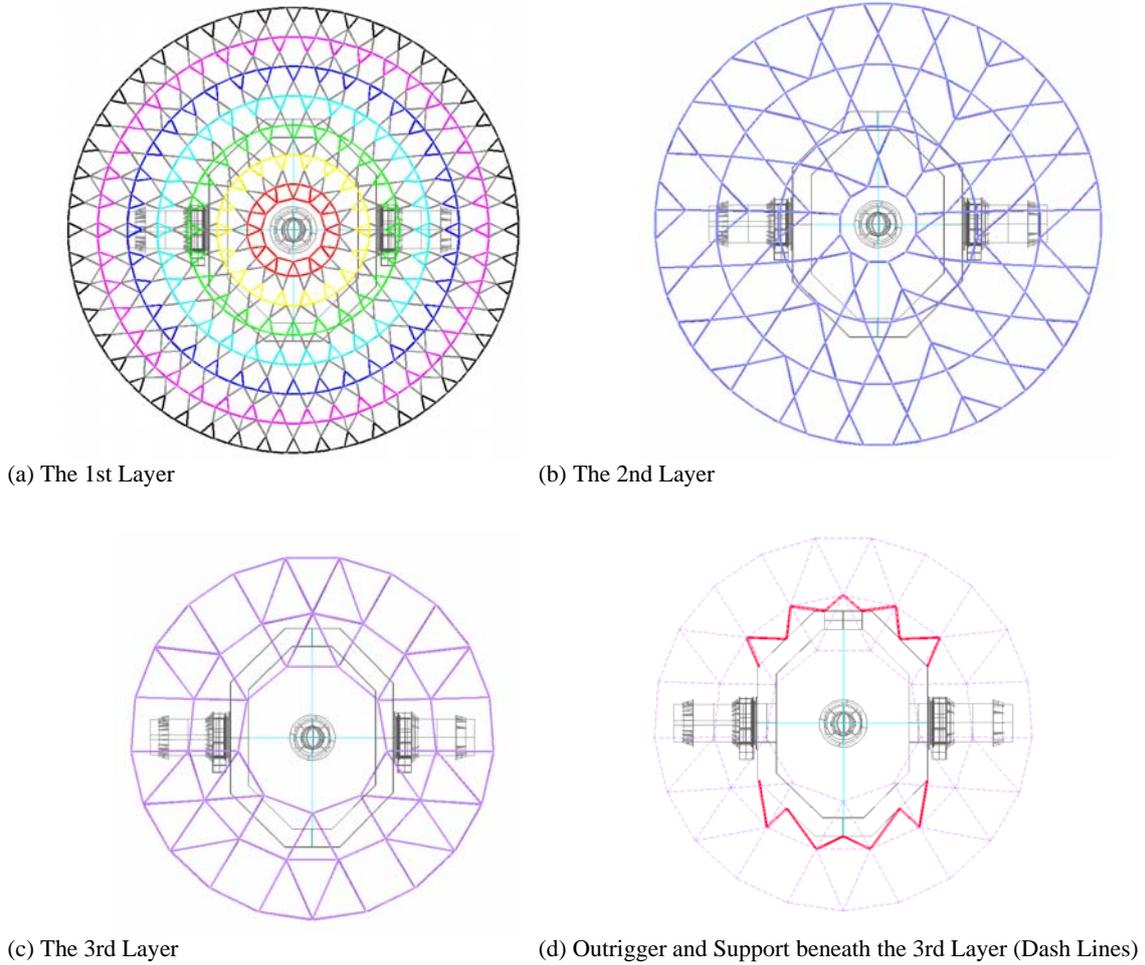

(a) The 1st Layer

(b) The 2nd Layer

(c) The 3rd Layer

(d) Outrigger and Support beneath the 3rd Layer (Dash Lines)

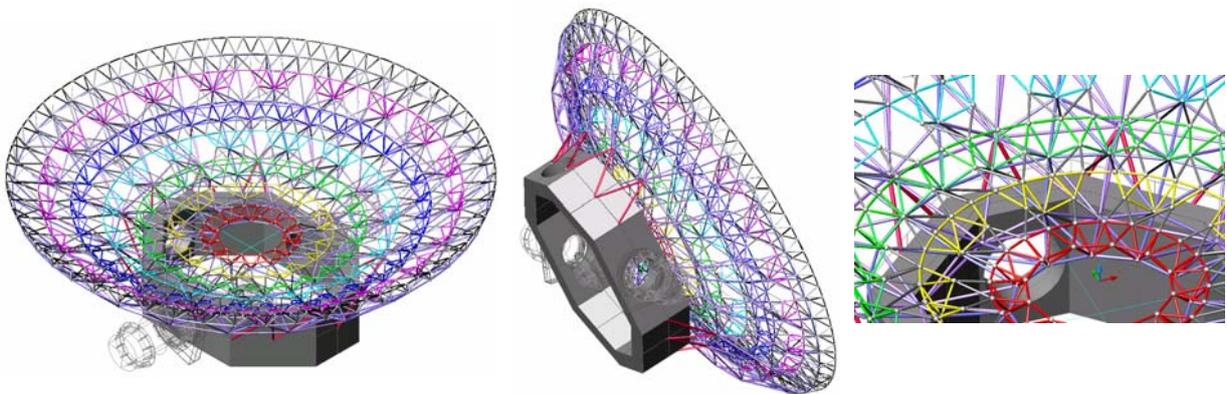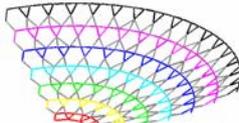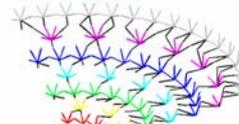Fig. 12. Projected Plans of the Space Frame Layers (Scheme 2)

Fig. 13. Computer rendering images of primary mirror support structure (Scheme 2)

Table 5. Configuration diagram of 1/3 space frame (Scheme 2).

	The 1st Layer	The same with Scheme1.
	Diagonals between the 1st and 2nd Layers	Two adjacent primary triangles are connected to one node in the 2nd layer. Member number is reduced by 17 %.
	The 2nd Layer	Unlike Scheme 1, the layer is not fully triangulated. Member number is reduced by 47 %.
	Diagonals between the 2nd and 3rd Layers	Two adjacent primary triangles are connected to one node in the 3rd layer. Member number is reduced by 49 %.
	The 3rd Layer	Not fully triangulated. Member number is reduced by 78 %.

In order to maintain stability of the space frame, the strategy to reduce number of bar members was composition of Platonic solid bodies. Fig 14 shows examples of Platonic solid bodies found in Scheme 2 space frame. Some of them appear complete bodies while the others are half or part of Platonic solid bodies. Because symmetry axes vary on each rings on the 1st layer, these platonic solid bodies are not ideal shapes, but skewed.
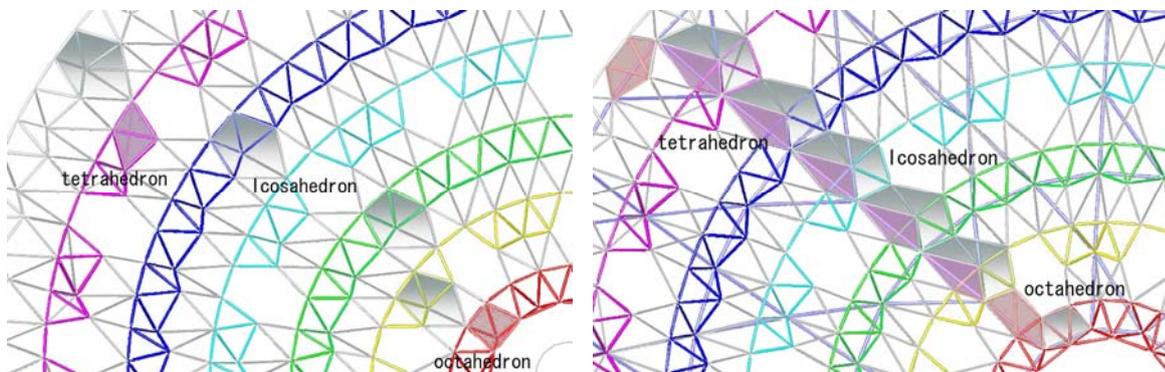
a) 1st Layer and 1-2 Diagonals

b) 1st Layer, 1-2 Diagonals and 2nd Layer
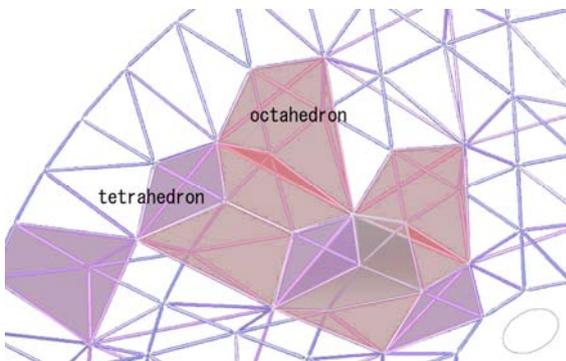
c) 2nd Layer, 2-3 Diagonals and 3rd Layer

Fig. 14. Complete or semi Platonic solid bodies that can be found in Scheme 2 space frame structure

The reduction in stiffness results in slightly lower natural frequency of the first mode as 5.4 Hz (Fig 18). Nonetheless, the relative deformations in the position of 75 degree tilt angle are still in the range of 4 mm in each component and 5 mm in magnitudes. See Fig. 15 to Fig.17 and Table 6. Table 7 shows that the nodal displacements of the 1st layer due to thermal gradient loads in Scheme 2 are greater, thought not significant, in most cases than those of Scheme 1 shown in Table 4. This indicates self-straining effects due to thermal gradients are reduced by lower degree of redundancy.

(a)   (b)

Fig. 15. Deformation due to gravity in Case 0 degree (Scheme 2) (a) Initial state (b) deformed state

(a)   (b)

Fig. 16. Deformation due to gravity in Case 75 degree (Scheme 2) (a) Initial state (b) deformed state

Table 6. Relative displacement due to gravity of Case 75 degree to Case 0 degree (Scheme 2)

Scheme 2	displacement vector (mm)		
	dx	dy	dz
max	1.94	-0.28	4.78
min	-2.08	-3.10	-3.19

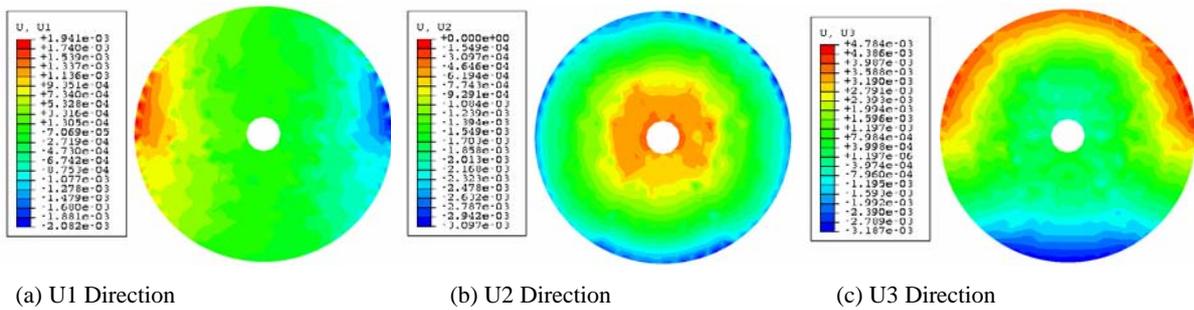(a) U1 Direction   (b) U2 Direction   (c) U3 Direction

Fig. 17. Relative deformation of the 1st layer (Scheme 2)

Table 7. Displacement Due to Temperature Gradients (Scheme 2)

	TL1			TL2			TL3			TL4		
	displacement (mm)			displacement (mm)			displacement (mm)			displacement (mm)		
direction	dx	dy	dz	dx	dy	dz	dx	dy	dz	dx	dy	dz
max	18.9	15.6	12.3	14.9	12.0	7.6	21.3	19.2	13.0	3.8	4.6	10.9
min	-21.2	-15.2	-12.1	-9.3	-10.4	-7.3	-23.2	-19.4	-16.4	-4.6	-3.3	-7.1

(a) Mode 1 (5.38 Hz)

(b) Mode 2 (5.92 Hz)

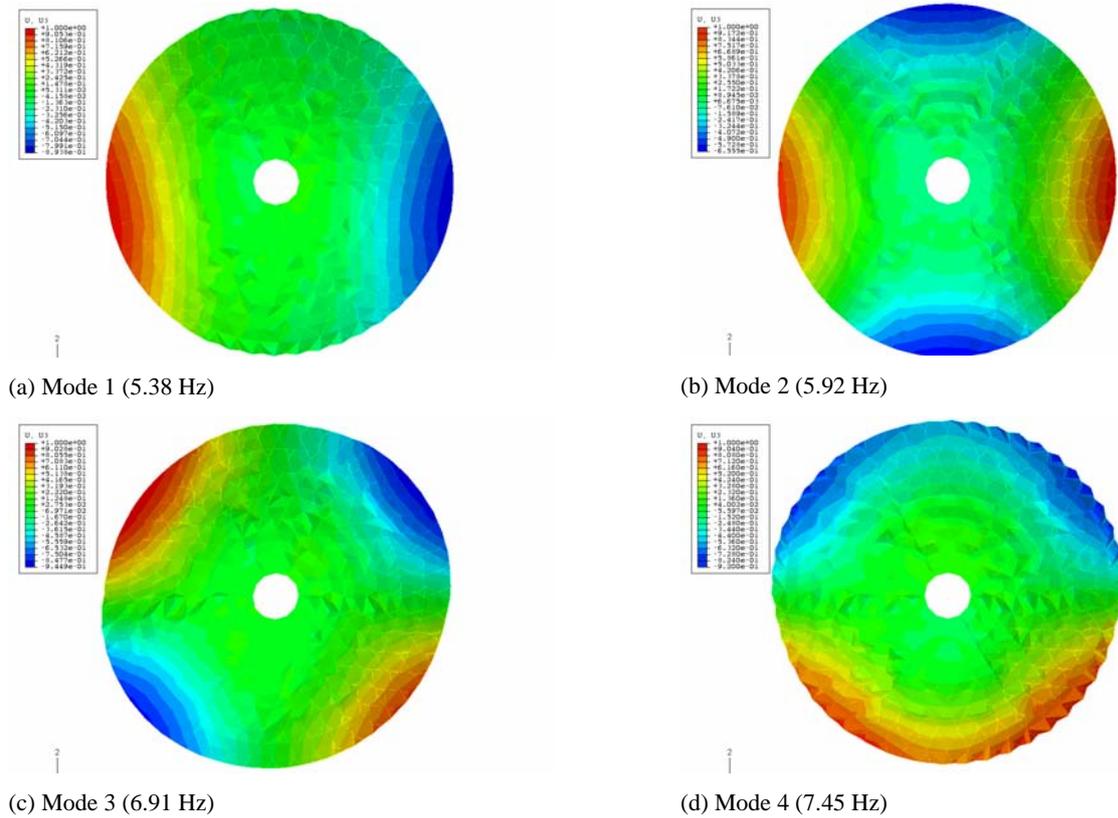(c) Mode 3 (6.91 Hz)

(d) Mode 4 (7.45 Hz)

Fig. 18. Natural vibration modes and frequencies (Scheme 2)

4. CONCLUSION

Two schemes for space frame arrangements are developed with acceptable stiffness and frequencies high enough, so potential vibrations do not reduce the image quality. Scheme 2 is preferable as to a lower grade of redundancy and less weight. What remains as a challenge is the warping of the surface due to thermal gradients. These deformations are in the real physical environment randomly distributed and unpredictable, and therefore absorb most of the resources for automatic adaption. Bars made from carbon fiber tubes would be preferred over steel tubes, because a primary mirror truss made with carbon fiber tubes would highly superior as to natural frequencies, stiffness, and thermal warping effects. The analysis and simulation of such a carbon fiber truss is one of tasks to be tackled in a future phase of the CCAT project.

5. REFERENCES

[1] *Foeppl,A.*: The Truss in Space; Pulishing House of B.G.Teubner, 1892

[2] *Mengeringhausen, M.:* Komposition im Raum (Composition in Space. The Art of Individual Building Shapes with Serial Elements); Bertelsmann 1983

[3] *Klimke, H.*: Geometric Optimization of Spatial Bar Structures with Computer Aided Design Tools. Bauingenieur 61 (1986), pp. 481-489

[4] *S. Stephan, Ch. Stutzki:* A General Method for the Design of Bolted Connections for Space Structures. In: Space Structures 5, Thomas Telford 2002